International Journal of Mechanical and Materials Engineering (IJMME), Vol.5 (2010), No.2, 175-181

PERFORMANCE AND FAILURE DURING ENERGY TESTING OF ZINC OXIDE VARISTOR PROCESSED FROM DIFFERENT POWDER SIZE FRACTION AND PASSIVATION THICKNESS

A. N. M. Karim[1], S. Begum[2] and M. S. J. Hashmi[3]
[1]Department of Manufacturing and Materials Engineering, International Islamic University
53100 Kuala Lumpur, Malaysia
[2]Department of Mechanical Engineering, Universiti Tenaga Nasional, Putrajaya, Malaysia
[3]School of Mechanical and Manufacturing Engineering, Dublin City University, Glasnevin, Dublin 9, Ireland
E-mail: Shahida@uniten.edu.my

Received 23 September 2010, Accepted 10 October 2010

ABSTRACT

The processing of ZnO varistor has a long route with numerous contributing variables. The role of particle size distribution in the starting powder is very crucial in varistor fabrication and performance evaluation. The varistors are also needed to be passivated before the evaluation of electrical performance. It was envisaged that the passivation thickness would influence the failure characteristics during energy testing as heat dissipation would be affected by the thickness. To investigate the above phenomena, the standard as produced varistor powder was fractionated to different narrow distributions containing large, medium and fine particles. Though there was no appreciable difference in physical properties but it was higher for discs fabricated with finer fraction of powder. However, the affect on green strength was quite reverse. In terms of electrical performance, the varistor discs with fine fraction of powder exhibited better properties though the energy absorption capability was poor. The variation of passivation thickness did not influence the energy absorption capability that much but the failure mode was changed. The higher thickness caused the failure by electrical puncture.

Key words: Particle size, Passivation thickness, Varistor, Energy absorption capability, Electrical punctures.

1. INTRODUCTION

A ZnO varistor is a semi-conducting device possessing a non-linear I-V characteristic with a symmetrical sharp breakdown similar to that of a zener diode (Matsuoka, 1971and Gupta, 1990). But unlike a diode, a varistor can limit over-voltages equally in both the polarities, thus giving rise to I-V characteristics which is analogous to the two back to back diodes. This has enabled it to provide an excellent transient suppression performance. It is a preferred approach to protect the electrical, electronic and power distribution and transmission circuits from destructive voltage levels induced by lightning impulse or switching surges over the past thirty years. Currently wide ranges of varistor products like high energy metal oxide varistors, multilayer surface mounted capacitors, industrial high energy metal oxide varistors etc. are available (Transient voltage suppression handbook, Harris, 1995 and Metal oxide varistor, downloaded 2010).

ZnO varistor is processed by the conventional powder processing route where the distribution pattern, as well as, the fraction percentage of each size influences significantly the particle arrangement and packing density, the size and the shape of the pore interstices, the deformation nature, sintering behavior and the microstructure developed during firing. The effect of the particle size distribution on sintering was observed by (Yeh and Sacks, 1988). They concluded that the green alumina compacts prepared from powders containing both narrow and wide size distribution can be sintered to high fired density without any exaggerated grain growth. However, the broad distribution will enhance the green density of compacts, and therefore, the shrinkage will be reduced to achieve the theoretical density. (Lange and Kellet, 1986) described the kinetics and transport theory for pore shrinkage with different packing arrangements and their dependence on the co-ordination number, ratio of the external surface energy to the grain boundary energy, short range and long range mass transport phenomena. The significant influence of the particle size on the tensile stress of the compacts made of aluminum and copper powders are observed by (German, 1977). (Duffield and Grootenhius, 1977) concluded that for optimal strength the fine powder with narrow distribution is necessary. Rumpf's theory (Rumpf, 1962) explains the effect of the particle size and packing on the green strength of the compacts, the influence of flaws on the green strength, describes the variability of strength, and interprets the effect of powder mixing, of environment and of sintering. Nano ZnO and Core shell type varistor powders were investigated by (Pillai et al, 2003) and found that core shell powder exhibited superior breakdown voltage than the commercial varistors samples prepared by simply mixing the nano ZnO and metal oxide. (Hingorani et al, 2003) have investigated ultrafine polycrystalline ZnO nanoparticles with size ranging

from 5–40 nm and concluded that a higher critical electric field and a higher coefficient of nonlinearity (α) in the logE *versus* logJ curve is achievable. It was also observed that by spray drying widely distributed zinc oxide varistor powder can be produced. The percentage of fine and coarse particles in the granules can be varied by controlling spray drying parameters and the widely distributed powder resulted from higher feed flow rate and lower atomization pressure would increase percent of coarse granules in the powder which would lead to higher compressibility and enhanced green density (Shahida and Hashmi, 2005). The performance of varistor was also affected by percent of fine and coarse granules present in the spray dried powder (Shahida et al., 2006). Though the nominal voltage was enhanced with higher percent of fine fractions, however, better energy absorption capability was achieved with increase fraction of coarse granules in the powder. (Patent 20100136337, 2010) stated that ZnO varistor powder in which 50% of the particle diameter in the range of 20-120μm can generates varistor with high operating voltage and excellent current-voltage nonlinear characteristics. ZnO varistor exhibited better electrical properties in terms of non-linear coefficient, breakdown voltage, leakage current and clamping voltage when prepared from powder produced by chemical synthesis (CS) than that of powder of mixed route (Lanyi et al, 2007).

In varistor fabrication the passivation thickness plays an important role. It is applied on the peripheral surface of the discs to provide a collar material and acts as a barrier to heat transfer during energy testing. US patent 4,046,847, US patent 3,959,543 and US patent 5,096,620 described different types of materials and its composition that can be used as passivating materials, whereas, patent 5,307,040 portrayed ceramic materials as passivating materials for MOV and observed degradation/deterioration or failure behavior of MOV block when subjected to an elevated temperature (120°-130° C) at an AC/DC bias with 10% above the maximum continuous operating voltage for at least 250-1000 hrs (US patent no: 5,307,040, 1994).

The present investigation was made to reveal the influence of different narrow size distribution of ZnO varistor powder in the fabrication of ZnO varistor and to compare with widely distributed varistor powder. It was found that narrowly distributed fine varistor powder could improve some physical properties but green strength was reduced compared to widely distributed powder. Some of the electrical properties were improved for varistor fabricated from narrowly distributed fine powder. However, energy absorption capability was poor for varistor of this category. As there was no study of the influence of glass thickness on the varistor performance, especially in terms of energy absorption capability, hence, the passivation thickness was varied at three levels and failure mode was also observed. The variation of passivation thickness did not have that much influence on the energy absorption capability; however, the mode of failure was changed.

2. EXPERIMENTAL PROCEDURE

The standard as produced powder was taken from production line and its particle size distribution is presented in Figure 1. It can be seen from the Figure that the particle size distribution is within the range of 45-150μm.

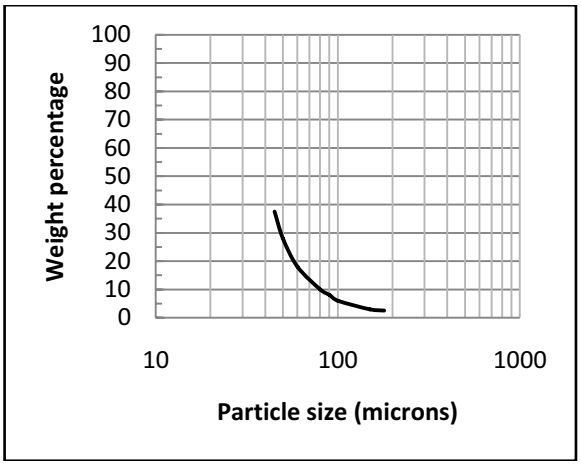

Figure 1 Particle size distribution of powder produced through the production scale dryer

The powder was fractionated to different narrow distributions containing large, medium and fine particles. A stack of sieves with 150, 90, 75 and 45 μm apertures was arranged successively from top to bottom. By placing the powder, the top most sieve was closed with a lid and secured tightly. The sieves were agitated for about 30 minutes and the fraction of powder on each sieve was collected. The powder was pressed using production compacting machine (Model HC-75EC, Hydramet American Inc., Royal Oak, Michigan). A target weight of 159.0 gm of powder was taken to produce green compacts of 38 mm in diameter. A standard pressing cycle was used and uniaxial double action compaction technique was adopted. The peak load applied to press three discs at a time was 25 ton leading to a pressure of about 75 MPa. Twelve blocks were pressed for each type of powder. Five samples from each type was used to measure the green strength and the rest compacted discs were sintered in the pot kiln with standard firing profile with a peak temperature of 1120°C. The fired bodies were passivated; their flat surfaces were ground and after ultrasonic cleaning and visual inspection for defects such as pinholes and damaged edges, the discs were electroded for performance evaluation. The identification of different size fraction is given in Table 1. To conduct the passivation test, samples of 32 mm fired diameter was collected from production line. Forty five discs were randomly grouped into three cells, fifteen in each. The glass thickness was varied by

passing through the glass spraying system. Thus the first cell was sprayed once, the second cell twice and the third cell thrice. After firing, the measurement of dimensions was carried out to estimate the glass thickness. After electroding, the discs were tested for energy absorption capability.

Table 1: Identification of different size fractions of powder

Type of powder	Size range (μm)
Cell A	150-90
Cell B	90-75
Cell C	74-45
Cell D	<45
Standard powder	150-45

2.1 Green Density and Strength

After pressing operation, the diameter, height and weight of the discs were measured to measure the green density. Green strength of the cylindrical compact was determined by diametral compression test. The discs were placed between two flat plates and load was applied with a speed of 5 mm/min. The green strength was calculated by using the following formula:

$$\sigma_g = \frac{2P}{\pi dh} \quad (1)$$

where, P is the load at fracture, d is the diameter and h is the height of the green disc.

2.2 Fired Strength

The mechanical strength of the sintered disc is very important for the electronic ceramics to achieve better electrical performance. It is envisaged that a disc with higher mechanical strength could be capable of withstanding more thermal stress due to temperature gradients. The energy absorption capability as well as high current performance can thus be enhanced. The strength was measured by diametral compression test as before, where the disc was placed in a fixture in between two flat plates and applying the load at a cross-head speed of 1 mm/min. The load of fracture was recorded and the strength was calculated using equation 1. Dimensions of the fired discs were used to calculate the strength.

2.3 Electrical Performance

The electrical performance was evaluated by measuring wattloss, nominal voltage and clamp ratio and energy absorption capability. The calculation procedure is described below. Wattloss is a measure of degradation, which was measured at 80% of the voltage at 1mA by using a Wattloss High Temperature Tester (Model no. LC-1201B, California Instruments, San Diego, CA). The degradation of varistor is a complex phenomenon which is considered to be function of barrier height, donor density, and breakdown voltage of the grain and grain boundary (Shen et al, 1993 and Brown, 2004). Varistors are required to sustain constant bias voltage in normal operation without significant degradation. Nominal voltage (also known as threshold, turn on, or non-linear voltage) is used to rate a varistor. This corresponds to the voltage at which the flow of current from linear to non-linear mode starts. Nominal voltage is evaluated from the following relationship:

$$E_{0.6} = \frac{V}{t} \quad (2)$$

where V is the voltage and t is the thickness of the device. The value of $E_{0.6}$ is controlled by the grain size and thus by the number of the grains. Clamping efficiency is a very important parameter defined as the ratio of voltages in the non-linear region. This parameter affirms the ability of a varistor to limit the transient voltage and the level of protection and is calculated as follows:

$$Clamping\ ratio = \frac{V_2}{V_1} \quad (3)$$

where V_2 is the voltage per unit length at a current density I_2 in the upturn region and V_1 is the voltage per unit length at current density I_1 at the onset of non-linear region. Non-linear co-efficient is the most critical parameter to characterize for zinc oxide varistor. The co-efficient, α is defined by the following formula:

$$A = d \ln I / d \ln V \quad (4)$$

The magnitude, therefore, varies with current density. It increases in the pre-breakdown region, attains a maximum value in the non-linear region and diminishes sharply in the upturn region.

The energy absorption capability of the varistors was performed in Haefely (Model no. WO 4435-36, Hipotronics Inc., Brewster, NY) impulse generator with capacity of 50 KV and 45 KJ. The generator produces square wave which consist of LC network of capacitor and reactor coils in between capacitors. The shape of the square wave is given in Figure 2. The energy absorption capability was calculated from the measured peak current and clamp voltage and the time duration by using the following relationship:

$$E = \int_0^t vidt = CVIt \quad (5)$$

where C is a constant and it depends on the wave shape of testing pulse. The value of V was taken in volt/cm, I in amp/cm^2 and t in seconds to calculate energy in $J.cm^3$. The energy absorption capability of varistors was measured by selecting a charging voltage for a fixed charging time. Three repeated shots of 2 ms square wave was applied for each cycle. The charging

voltage was selected at a low level so that no failure occurs in the first cycle. The cycle of shot continued until all of the discs of the sample failed. The value of clamp voltage and peak current for each shot was recorded. The cumulative curve of energy absorption was plotted from the calculated energy and the number of discs failed at that energy level.

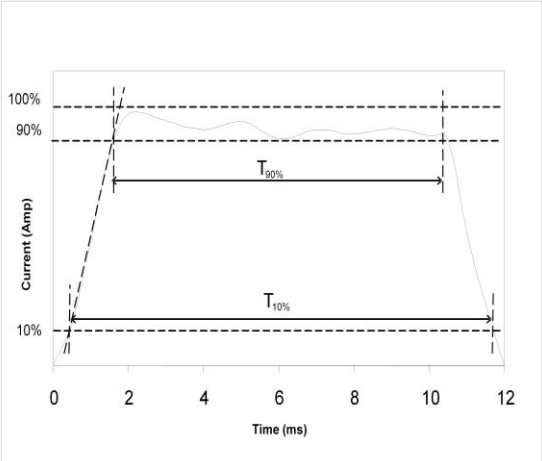

Figure 2: The shape of square wave current applied to evaluate energy absorption capability

3.0 ANALYSES AND DISCUSSIONS

3.1 Physical Characterization of Varistor with Different size Fraction of powder

The physical characteristics of discs prepared from the powder with narrow distribution of different size ranges and the standard one are presented in Table 2. The values within parenthesis are standard error. The green and the fired density did not show any appreciable difference but these are highest for cell D which had particle size smaller than 45 μm.

Table 2: Physical characteristics of discs produced from powder with different narrow size range

Powder type	Green density (gm/cc)	Fired density (gm/cc)	Green strength (MPa)
Cell A	3.380± (0.03)	5.60±(0.011)	0.89± (0.01)
Cell B	3.387± (0.01)	5.60±(0.014)	0.91± (0.02)
Cell C	3.332± (0.02)	5.58±(0.028)	0.92± (0.03)
Cell D	3.389± (0.04)	5.62±(0.015)	0.76± (0.03)
Standard	3.334± (0.03)	5.59±(0.021)	0.91± (0.03)

The enhanced fired density was achieved as a result of higher capillary pressure exerted by the liquid formed during sintering. The total surface energy was also higher due to the small radius of curvature. Both the capillary pressure and surface energy provide more driving energy for densification. The green strength was lowest with cell D, while it was almost the same for all the other cells including the standard one. According to Rampf's theory (Rampf, 1962) higher green strength was thought to be obtained from the powder containing smaller particles. However, it is predicted that due to frictional effect the packing of the particles was not effective which reduced the strength.

3.2 Electrical Characteristics of Varistor with Different size Fraction of Powder

The electrical properties were evaluated for the varistors fabricated from the powder of different size ranges including the standard distribution. The clamp ratio, non-linear coefficient (α), and wattloss are summarized in Table 3. The clamp ratio and α did not change significantly for different cells. The clamp ratio was slightly higher and the nonlinear coefficient was lower for cell D. The wattloss before the application of the high amplitude short duration pulses of peak current 65 KA was found to be slightly higher for the same cell. But after the application of the high current pulses, increment in wattloss was minimum for cell D making it comparable with varistors from all other cells. The electric field strength of varistor produced from powder having different size ranges is plotted in Figure 3. The lowest was achieved for cell A and highest for cell D. The effect of particle size is clearly evident from the plot as cell A was composed of coarser particles and cell D of finer particles. It can be inferred that the coarser spray dried granules lead to bigger grains after sintering leading to lower nominal voltage. The finer granules generate smaller grains after firing.

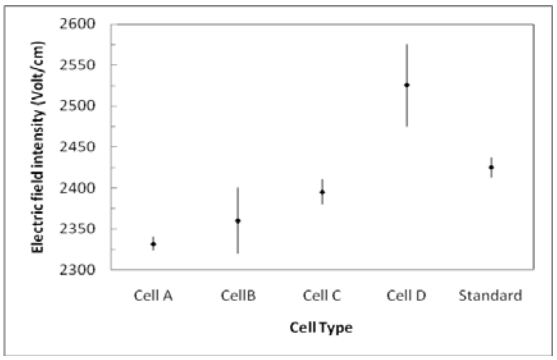

Figure 3: Electrical field strength of varistors produced from powders with different size fractions

The energy absorption capability of varistors prepared from the powder containing particles of different size ranges is illustrated in Figure 4. It is evident that the energy withstanding capability is low for cell D. The other fractions composed of coarse, medium and wide distribution of particles do not exhibit any noticeable difference. It can be said from the data presented in Table 2 that the green body is less homogenous for cell

D. The inhomogeneity of the discs in the green state might be intensified further by firing. Hence the varistor failed at very low level of injected energy.

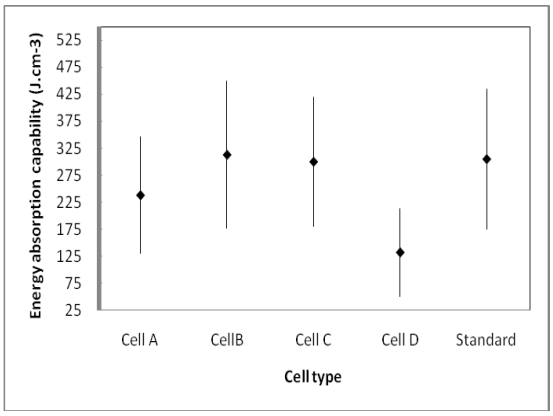

Figure 4: Energy absorption capability of varistors produced from the powders with different size fractions

The failure mode of varistors by the destruction testing is presented in Table 4. It is noticeable from Table that the failure occurred mainly by flashover and by combined flashover and pinhole. The variance analysis for the cell D and the standard one was carried out considering the energy absorption capability as the response and it is presented in Table 5. The calculated F-statistics at 95% confidence interval was higher than F_{tab} at $\gamma_{1,19}$. Therefore, it can be said that the particle size fraction exhibited a significant influence on the energy absorption capability of the varistors.

3.3 Passivation Thickness

The glass thickness plays an important role in varistor performance. The influence of glass thickness on varistor performance was assessed by evaluating the energy absorption capability.

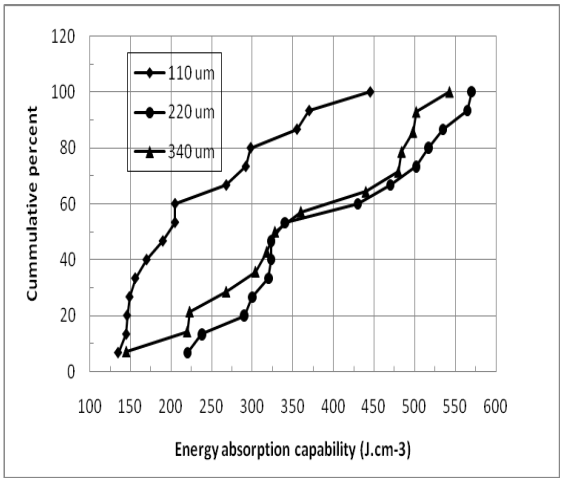

Figure 5: Energy absorption capability of varistors having different glass thicknesses

The cumulative plot of the energy absorption capability of the varistors with different glass thickness is presented in Figure 5 and the mean energy with standard error is illustrated in Figure 6. The standard amount of glass taken as the minimum level in the experiment had shown inferior performance and the varistor started to fail at very low energy level. Nevertheless, the heaviest coating did not exhibit the best energy absorption capability.

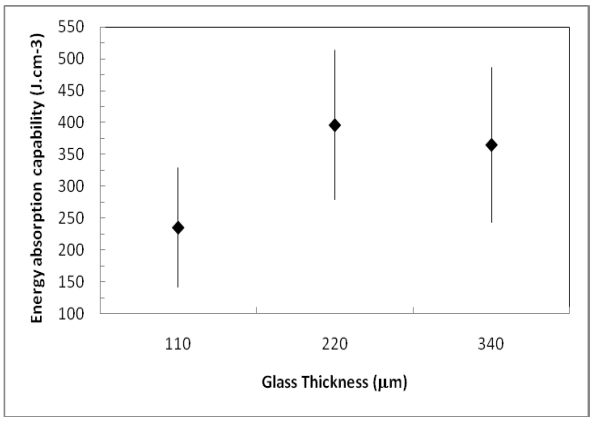

Figure 6: Mean value of energy absorption capability with ± standard deviation of the varistors having different glass thicknesses

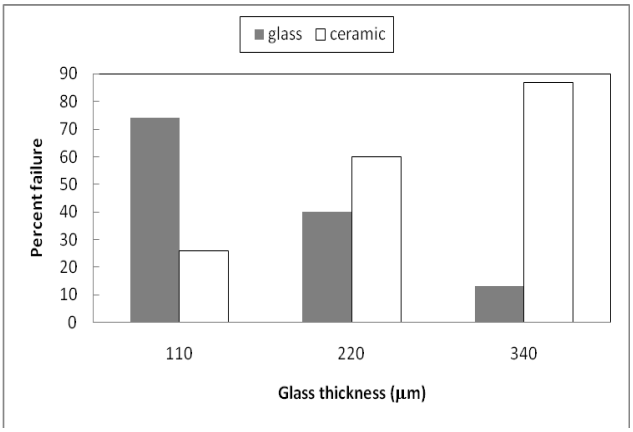

Figure 7: Failure mode of the varistors during destruction testing having different glass thicknesses

The coating of the glass acts as an insulator and resists the heat transfer. The effect is more obvious in the second and third shot in the energy test. The heavier coating acts as higher insulator and does not dissipate heat as effectively as the lower thickness. Thus the high temperature in the ceramics makes it more vulnerable to failure. This feature is supported by the fact that the thicker coating failed through the ceramic and most of the discs failed by electrical puncture as presented in Table6. It is also noticed from Figure 5 that for the best cell, 50% of the discs survived after 400 $J.cm^{-3}$. The mode of failure was also categorized and illustrated in Figure 7.

Table 3: Clamp ratio, non-linear co-efficient and wattloss for varistor fabricated with different size fractions of powder

Cell identification of varistors	Non-linear co-efficient (α)	Clamp ratio	Wattloss ($W.cm^{-3}$)		
			Before shot	After shot	
	@ 1mA-5 mA	@5mA-5KA		Forward polarity	Reverse polarity
Cell A	15.041	1.693	0.010	0.011	0.013
Cell B	14.682	1.694	0.009	0.012	0.015
Cell C	14.498	1.692	0.009	0.011	0.013
Cell D	14.189	1.702	0.012	0.012	0.015
Standard	14.175	1.696	0.009	0.011	0.014

Table 4: Failure pattern during "strength to destruction" testing for varistors fabricated with different size fractions of powder

Cell identification	Sample size	Failure mode			
		Pinhole (ph)	Flashover (fo)	Ph+fo	Ph+crack
Cell A	16	3	5	8	-
Cell B	11	2	5	3	1
Cell C	15	2	5	8	-
Cell D	6	3	2	1	-
Standard	15	1	8	6	-

Table 5: Analysis of variance for the energy absorption capability of varistor with different size fractions of powder

Source of variation	Sum of squares	Degrees of freedom	Mean squares	F_{cal}	F_{tab}
Treatment	92107	1	92107		
Error	337710	19	17774	5.18	4.38
Total	429817	20			

Table 6: Failure mode of varistors with different glass coatings during "strength to destruction" test

Glass Thickness (μm)	Sample size	Failure Mode						
		Inter-face	Pinhole(ph)	Flashover (fo)	Rupture	Interface+ fo	Interface + ph	ph+fo
110	15	8	3	-	-	3	-	1
220	15	3	4	-	4	3	-	1
340	14	-	8	-	2	2	-	2

Table 7: Analysis of variance for the energy absorption capability of varistor with various glass thicknesses

Source of variation	Sum of squares	Degrees of freedom	Mean squares	F_{cal}	F_{tab}
Treatment	225721	2	112861		
Error	469384	41	11448	9.858	3.234
Total	695105	43			

It is clear from the Figure that the increase of glass thickness has shifted the failure. More than 85% of the varistors failed through the ceramic coated with thicker passivation coating compared to 27% in the case of the thin coating. The variance analysis of the varistors with different glass thickness is given in Table 7. At 95% confidence interval the tabulated F-statistics at $\gamma_{2,41}$ is less than F_{cal}. Hence the glass thickness has significant influence on the energy absorption capability of the varistor.

4.0 CONCLUSIONS

Insignificant effect of different particle size fractions was observed on the physical properties of the discs and the performance of the varistor. Though there was a high frictional effect with the fine fractions, but it could produce discs with higher green density in comparison to a widely distributed standard powder. However, a reduction in the green strength was observed. The fired density was also higher for the fine fraction of powder. The particle size fractions had a significant influence on the nominal voltage and the energy absorption capability of the varistor. A higher nominal voltage was obtained when the varistor was fabricated from the fine fraction of powder. Degradation of varistors made from the fine fraction of powder was found to be less after the application of the high amplitude short duration pulses. Nonetheless, the energy absorption capability was degraded severely. Hence on the basis of physical characterization and evaluation of the electrical performance it can be said that the powder with a wide distribution is more suitable for the fabrication of zinc oxide varistor. A significant influence of glass thickness on the energy absorption capability left the scope of optimizing the amount of glass to be used for passivating. Neither too low nor too high amount of passivating material is favorable for varistor performance. Initial failure was prevented by applying glass material of thickness of 220 μm and survival of a larger number of discs above 500 J. cm^{-3} was also increased.

Acknowledgements

This work was carried out as a part of the DOCERPO project within the BRITE/EURAM II program. All the research activities were conducted in Harris Corporation, Semiconductor Division, Dundalk, Ireland and the authors gratefully acknowledge the materials and testing facilities provided by them.

REFERENCES

Begum, S. and Hashmi , M.S.J., 2005. Effect of Spray Drying Variables on the Characteristics of ZnO Varistor Powder, Proceeding for IATC2005, 6-8 December, UPM, Malaysia, 59-67.

Begum, S , Karim, A.N. M and Hashmi, M.S.J. , 2006, Performance Evaluation Zinc Oxide Varistor Produced from Powder under Different Spray Drying Conditions, Proceeding of the International Conference of Manufacturing Materials, ICMM2006 , Malaysia, 272-277.

Brown K., 2004, Metal Oxide Varistor Degradation, http://www.iaei.org/magazine.04 b brown.htm, March/April, down loaded 24/09/10.

Duffield, A, and Grootenhuis, P., 1977, J. Inst. Metals, 87, 33.

German, 1977, Strength Dependence on Porosity for P/M Compacts, Int. J. Powder MET. Powder Tech, 13 (4), 259-71.

Gupta, T. K., 1990, Application of Zinc Oxide Varistors, J. Am. Ceram. Soc. 73(7), 817-1840.

Hingorani, S., Pillai, V., P. Kumar, et al, 2003, Micro emulsion Mediated Synthesis of Zinc-oxide Nanoparticles for Varistor Studies, Materials Research Bulletin, 28 (12), 1303-1310.

Matsuoka, M., 1971, Non-ohmic Properties of Zinc Oxide Ceramics, Jpn. J. Appl. Phys., 10(6), 736-46.

Metal Oxide Varistor: Littlefuse Voltage Suppression,http://littlefuse.com/metal_oxide_varistor.html, Downloaded 24/09/10.

Lange F. F, and B. Kellet, 1986, Influence of Particle Arrangements on Sintering, Proceeding on Science of Ceramic Chemical Processing, Wiley Interscience Publication, NY, 561-576.

Lanyi, W., Chengxiang, L., and Guoyi, T., 2007, Fabrication of High performance Multilayer ZnO Varistors with Chemically Synthesized Doped Zinc Oxide Powder, Key Engineering materials, Trans Tech Publications, Switzerland, 336-338, 739-742.

Patent: 21200136337, 2010, "ZnO Varistor Powder", 24/09/2010.

Pillai, S. C, Kelly, J. M, et al, 2003, The Effect of Processing Conditions on Varistors Prepared from Nanocrystalline ZnO, J. Mater. Chem. 13, 2586-2590.

Rumpf, H., 1962, The Strength of Granules and Agglomerates, International Symposium on Agglomeration, Edited by W.A. Knepper, Interscience, London, 379-418.

Shen, C. Y. Chen and L. Wu,, 1993, The Effect of Antimony Oxide on the Electrical Properties of ZnO Varistors, J. Appl. Phys., 32, 1147-1153.

Transient Voltage Suppression Devices 1995, A Data book published by Harris Semiconductor, Melbourne, FL 32902, USA.

Yeh, T., and Sacks, M. D, 1988, Effect of Green Microstructure on the Sintering of Alumina, 90th Annual Meeting and Exposition, Cincinnati, Ohio, May1-5.

US patent no: 5,307,040, April26 1994, Down loaded 24/09/10.